Journal of Medical Devices Technology
jmeditec.utm.my

Original Research

On-Body Reduced Size AMC Design for Lowering Specific Absorption Rate in Wearable Antenna Application

Biragathis Babu[1,3], DiviyaDevi Paramasivam[1], Raimi Dewan[1,2,3*], Noor Asmawati Samsuri[1] and Nazirah Othman[1]

[1] *Advanced Radio Frequency & Microwave Research Group, Faculty of Electrical Engineering, Universiti Teknologi Malaysia, 81310 UTM Johor Bahru, Malaysia*
[2] *IJN-UTM Cardiovascular Engineering Centre, Institute of Human Centered Engineering, Universiti Teknologi Malaysia, 81310 UTM Johor Bahru, Malaysia.*
[3] *Department of Biomedical Engineering and Health Sciences, Faculty of Electrical Engineering, Universiti Teknologi Malaysia, 81310 UTM Johor Bahru, Malaysia*

ARTICLE INFO

Article History:
Received 1March 2024
Accepted 28 June 2024
Available online 30 June 2024

Keywords:
AMC,
coplanar waveguide antenna,
gain,
metamaterial,
SAR

ABSTRACT

This manuscript investigates the design parameters of an Artificial Magnetic Conductor (AMC) and their impact on the Specific Absorption Rate (SAR) when integrated with a Coplanar Waveguide (CPW) antenna. The AMC was designed with periodic square patches of 10 mm x 10 mm on a grounded dielectric substrate with a thickness of 1.6 mm and a dielectric constant of 4.4. The AMC design was optimized using CST Microwave Studio to achieve a 0-degree reflection phase at the operational frequency of 2.4 GHz. The optimization process involved varying the dimensions of the patches and the spacing between them to minimize return loss and maximize radiation efficiency. The CPW antenna, with and without the AMC, was simulated in the presence of a realistic human chest model to evaluate SAR levels. The results indicate that the introduction of the AMC improved the impedance matching of the antenna, reducing the reflection coefficient (S11) from -10 dB to -20 dB at 2.4 GHz. Furthermore, the integration of the AMC increased the antenna gain from 2 dBi to 5 dBi. Most importantly, the peak SAR value in the human chest model was reduced from 1.8 W/kg to 0.8 W/kg over 1g of tissue, demonstrating the AMC's effectiveness in lowering RF exposure to human tissues. These findings highlight the potential of AMCs in enhancing the performance and safety of wearable wireless devices by effectively reducing SAR levels while improving antenna efficiency.

INTRODUCTION

Wireless Body Area Networks (WBANs) have become increasingly important in recent years due to their potential applications in various fields such as health monitoring, rescue services, military communications, and wireless computing (Asif et al., 2019). The performance of WBANs heavily relies on wearable antennas, which play a vital role in these networks. However, the proximity of these antennas to the curved human body poses challenges and has drawn significant attention from both researchers in academia and industry (Othman et al., 2020, Alù et al., 2007, Asif et al., 2019).

Wearable antennas must meet specific criteria to ensure effectiveness in functionality. They need to be flexible, durable, small in size, low-profile, lightweight, comfortable to wear, and able to conform to the contours of the human body. The coupling between the antenna and the body can alter the operating frequency, radiation efficiency, and radiation pattern of the wearable antenna. Adhering to Specific Absorption Rate (SAR) guidelines is crucial to minimize the electromagnetic impact on the body (Othman et al., 2020). One approach to improve the performance of wearable antennas is through the incorporation of metamaterials (Ali et al., 2023). Metamaterials, engineered materials with properties not found in naturally occurring substances, can be designed to have unique electromagnetic properties that enhance antenna performance. These materials can be tailored to achieve specific characteristics such as negative permittivity or permeability, which can be exploited to

* Raimi Dewan (raimi.dar@utm.my)

Department of Biomedical Engineering & Health Sciences , Faculty of Electrical Engineering, Universiti Teknologi Malaysia, 81310 UTM Johor Bahru, Johor, Malaysia.

improve antenna efficiency, bandwidth, and reduce SAR in wearable applications (Zhang et al., 2022).

An Artificial Magnetic Conductor (AMC) can be considered a type of metamaterial due to its unique electromagnetic properties and engineered structure. Metamaterials are artificial materials that exhibit properties not found in naturally occurring substances. Miniaturized AMCs enable the development of portable and lightweight systems, making them more convenient for users to carry or wear (Alù et al., 2007).

The choice of 2.4 GHz as the operating frequency for the CPW antenna with integrated AMC in this study is driven by regulatory availability, favorable propagation characteristics, the balance between antenna size and performance, and the extensive research and development resources available for this frequency band (Asif et al., 2019). These factors collectively ensure that the antenna can be efficiently integrated into wearable devices, providing reliable and efficient wireless communication while meeting global standards and regulations.

Some research indicates that antennas integrated with AMC can effectively reduce SAR levels through the manipulation of the electromagnetic field. For instance, they designed a monopole antenna operating at 2.45 GHz, incorporating a 5 by 5 grid of AMC unit elements (Ashyap et al., 2019,). Their investigation revealed that the SAR values, when averaged over a 10-gram tissue sample situated just 1 millimeter away from the tissue model, were only 0.18 W/kg and 0.371 W/kg, respectively (Babu et al., 2021,). Another study introduced a wearable antenna featuring an M-shaped monopole design with a 3 × 3 AMC structure (Bacova & Benova, 2022). This incorporation of the AMC structure resulted in a 3.7 dBi gain improvement, coupled with a substantial 64% reduction in SAR values.

This paper proposes a miniaturized AMC, incorporating with 2.4 GHz CPW antenna. The incorporation of AMC to the antenna was studied with parameters that significantly change such as reflection coefficient, gain, radiation pattern, and SAR values. This will prove that the incorporation of AMC to the antenna can improve the antenna's performance and reduce the SAR values (Balanis, 2016).

METHODOLOGY

Design Consideration

The AMC's design should match the frequency range of the antenna system it's intended to work with. The geometrical features of the AMC, such as unit cell dimensions and periodicity, should be tailored to the operating frequency for optimal performance. The miniaturization of an AMC using the reflection phase method involves reducing the physical size of the AMC structure while maintaining its desired reflection phase response at 2.4 GHz (Choudhary et al., 2020). AMCs are designed to operate at a specific resonant frequency, f. At this frequency, the AMC exhibits its characteristic behaviour (such as a reflection phase of 0 degrees). The resonant frequency f is related to the physical dimensions of the AMC unit cells and their periodicity, which are typically on the order of a fraction of the wavelength λ. This formula used to design and help to miniaturized the AMC structure.

$$c = f\lambda$$

where:

- c is the speed of light in a vacuum (approximately 3×10^8 meters per second),
- f is the frequency of the electromagnetic wave,
- λ is the wavelength of the electromagnetic wave.

Antenna and AMC Design Evolution

The simulation of the antenna and AMC structures are performed using CST Microwave Studio. The Coplanar Waveguide (CPW) antenna is compared to the literature as in Table 1. In the existing research papers, antenna is integrated with an AMC surface. This innovation was designed for operation at 2.4 GHz and utilized various substrate materials. To the best of our knowledge, no prior research has been published regarding the development of an antenna for wearable applications using a medical transdermal patch as the substrate (Bora et al., 2020). Additionally, the proposed antenna-AMC exhibited a smaller width in proportion to its overall dimensions and achieved a higher antenna gain compared to the previous works as shows in Table 1. The selection of Polycarbonate as the substrate for the CPW antenna with integrated AMC was driven by its balanced dielectric constant, low loss tangent, mechanical stability, and compatibility with AMC structures. These factors collectively contribute to optimizing the antenna's performance at 2.4 GHz, ensuring high efficiency, effective impedance matching, and significant SAR reduction, which are critical for safe and efficient wearable device applications. For wearable antennas and applications where flexibility and biocompatibility are paramount, Kapton and Medical Transdermal Patch are the most suitable substrates. Kapton offers excellent electrical properties, flexibility, and mechanical strength, making it ideal for high-performance wearable devices. Medical transdermal patches are highly biocompatible and flexible, perfect for direct skin contact but may not be suitable for high-performance electronic components due to their variable dielectric properties.

Vinyl provides a balance between flexibility and biocompatibility but may have higher dielectric losses. Polycarbonate offers good mechanical strength and moderate flexibility, making it suitable for some medical devices, although not as ideal as Kapton for flexible electronics.FR4 and Rogers RO4003C are less suitable for flexible and wearable applications due to their lower flexibility, despite their excellent electrical properties and mechanical strength.

Table 1 Proposed antenna-AMC with integrated antenna-AMC in literature

Frequency (GHz)	Gain (dB)	Type flexible substrate	Reflect plane	Dimension (λ × λ)	SAR (W/kg)	Refs.
2.40	8.06	FR-4	AMC	0.12 × 0.12	0.90	(Bora et al., 2020,)
2.45	6.40	Rogers	AMC	0.7 × 0.66	0.29	(Chen et al., 2019,)
2.45	5.20	Polyamide	AMC	0.58 × 0.58	0.30-3.89	(Choudhary et al., 2020)
2.45	7.40	Polyamide Kapton and vinyl	AMC	0.23 × 0.23	0.15	(Christina, 2022,)
2.45	4.90	Medical transdermal patch	AMC	0.36 × 0.06	0.53	(Chuquitarco-Jimenez et al., 2021)
2.40	7.10	Polycarbonate	AMC	0.17 × 0.17	0.20	(Das et al., 2020)

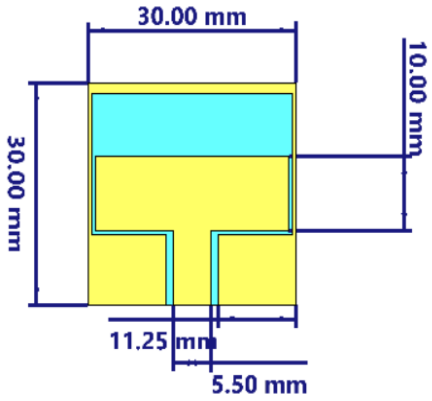

Fig. 1. Design of CPW antenna

This paper proposed the miniaturized AMC that is used to enhance the gain of CPW-fed antenna. In this work, performance comparison between the CPW-fed antenna with and without AMC is discussed. The result of return loss, realized gain and radiation pattern are also presented. CPW with and without AMC incorporation is discussed. Figure 1 shows the antenna's design from the front view. The FR-4 substrate with a thickness of 0.5 mm, a relative permittivity of 4.4, and a loss tangent of 0.02 is used for the antenna. The size of the CPW antenna is 12 mm and 36 mm respectively. The design and simulation of the antenna is performed in Microwave Studio (CST) software.

The proposed design of the planar AMC unit cell is shown in Figure 2(b). The unit cell comprises of two symmetric patches, each with two arms. The unit cell is simulated on polycarbonate substrate with a height of h = 0. mm, loss tangent of 0.001 and a dielectric constant εr of 3.

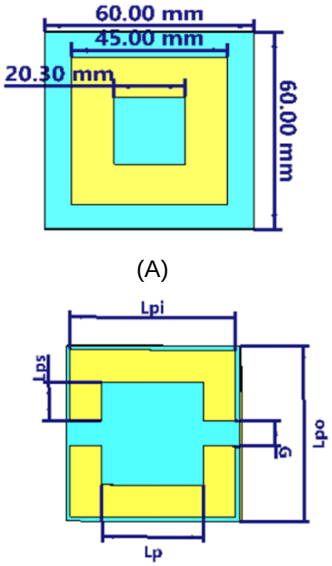

Fig. 2. Development of proposed AMC structure from (A) the initial design and (B) the finalized design of AMC unit cell with reduced in size.

The size reduction of an AMC unit cell involves reducing the physical size of the AMC structure while maintaining its desired reflection phase response at 2.4 GHz. The first step is to optimize the design of the AMC structure. This involves selecting the appropriate unit cell geometry, especially the dimensions of Lp and G. The parameter of Lpo is outer layer of the substrate, Lpi is the length of outer patch, Lp is the length of the inside patch, ts is the thickeness of the substrate and G is the gap the between of the two patches. After alternating the length of parameters, Lp and G shows it can lead to a shift in its resonance frequency. This shift might affect the desired operating frequency of the antenna system, potentially causing a mismatch between the antenna and the AMC.

Table 2 List of parameters of the proposed AMC design

Length	Value	Description
Lpo	21 mm	Length
Lpi	20 mm	Length
G	2 mm	Length
Lp	12.30 mm	Length
ts	0.50 mm	Thickness
Lps	4.65 mm	Length

In this study, the parameters of the Artificial Magnetic Conductor (AMC) design were outlined as shown in Table 2. The outer length (Lpo) of 21 mm and the inner length (Lpi) of 20 mm were critical for setting the size and resonant frequency of the AMC unit cell. The gap (G) of 2 mm between patches influenced the electromagnetic interactions within the AMC structure. The length (Lp) of 12.30 mm and another length parameter (Lps) of 4.65 mm contributed to achieving the desired resonance and reflection properties. The substrate thickness (ts) of 0.50 mm was essential for maintaining the dielectric properties and performance stability of the AMC.

Figure 3 shows the human voxel model in CST software. The human voxel model was segmented, as shown in Figure 3 to obtain accurate and reliable results in electromagnetic simulations. It ensures a realistic representation of the human body, enables the assignment of spatially varying material properties, facilitates SAR evaluation, improves accuracy in field distribution, and allows for targeted analysis of electromagnetic effects on specific body regions. Moreover, segmenting the human voxel model to simulate the region of interest (ROI) reduce the simulation time.

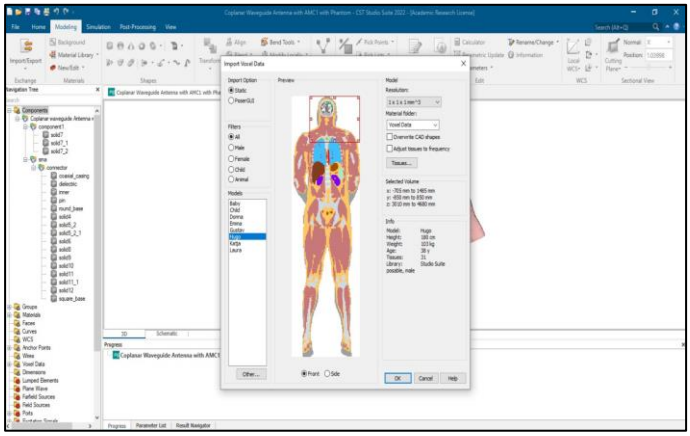

Fig. 3. The segmentation of human model

RESULTS AND DISCUSSION

The Conventional CPW antenna was tested on free space to ensure it resonated at 2.4 GHz. Its performance was evaluated

by assessing parameters such as the reflection coefficient (S11) and radiation pattern. Following this, the AMC was designed in a free space environment, with a focus on studying its reflection phase and optimizing its configuration. Subsequently, the designed antenna was placed on a human chest voxel model available in CST Studio Licensed Version 2022. The results of the SAR analysis conducted on the antenna, both with and without the inclusion of the AMC, are presented and discussed in this section. Additionally, the gap between the antenna and the voxel body was examined. To enhance comfort and user-friendliness, miniaturization of the AMC was performed, aiming for improved performance characteristics when reducing its size. This miniaturization ensures that these devices can be worn comfortably without causing discomfort or hindrance to the user.

The design process of the Artificial Magnetic Conductor (AMC) underwent several stages to optimize its performance and achieve a significant reduction in size while maintaining the desired electromagnetic properties. Initially, the AMC unit cell featured a basic structure with key parameters such as the outer length of the patch (Lpo), the length of the inner patch (Lpi), the gap between the patches (G), the length of the inside patch (Lp), the thickness of the substrate (ts), and another critical length (Lps). In its initial phase, the dimensions of these parameters were relatively large, resulting in a bigger AMC unit cell.

During the optimization phase, the primary objective was to reduce the physical size of the AMC while ensuring effective operation at the desired frequency of 2.4 GHz. This involved adjusting parameters like Lp and G, with iterative modifications to observe changes in the reflection phase and ensure that the AMC maintained a reflection phase of 0 degrees at the target frequency. Each iteration included simulations using CST Microwave Studio to study the reflection phase and electromagnetic behavior of the AMC unit cell.

After numerous iterations and adjustments, the final design of the AMC was achieved, significantly reducing the size of the unit cell by 67% compared to the initial design. This optimized design ensured minimal mismatch and effective operation at 2.4 GHz. The miniaturized AMC unit cell was crucial for enhanced integration into wearable devices, improved user comfort, and effective reduction of Specific Absorption Rate (SAR), ensuring safer interaction with human tissue by minimizing electromagnetic absorption. The final design parameters included Lpo at 21 mm, Lpi at 20 mm, G at 2 mm, Lp at 12.30 mm, ts at 0.50 mm, and Lps at 4.65 mm, successfully meeting the requirements for a compact, efficient, and safe solution for wearable antenna applications.

The Effect of Dimensions on AMC Characteristics

The miniaturization of an AMC for operation at 2.4 GHz stems from the need to ensure efficient electromagnetic field manipulation while maintaining compatibility with prevalent wireless communication standards. Figure 3 depicts the reflection phase of AMC at 2.4 GHz.In practical applications, the reflection phase of an AMC spans from +180 to -180 degrees across the frequency range, crossing zero at the operating frequency. The useful bandwidth (BW) of the AMC is defined as the range between +90 and -90 degrees on either side of the central frequency (0 degrees) as the lower frequency and higher frequency respectively.

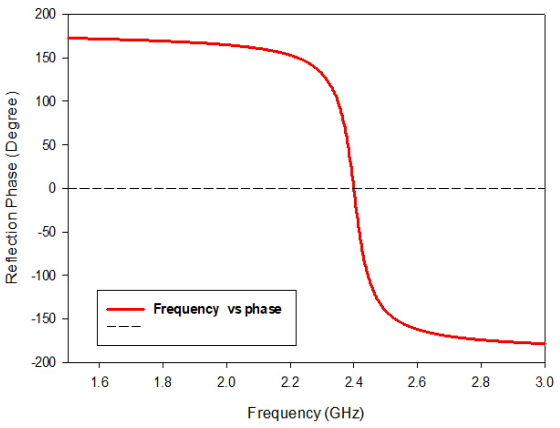

Fig. 4. Reflection phase of AMC 2.4 GHz

Based on the results shown in Figure 4(a) it is observed that reducing the Lp value leads to a minor shift in the operating frequency of the AMC.The reflection phase of an AMC changes when the length of the AMC structure is altered from 12.0 mm to 12.6 mm. The reflection phase is a critical parameter that determines how electromagnetic waves are reflected from the AMC, affecting its performance and interaction with incident waves.

When the length of Lp of the AMC structure is increased or decreased, it influences the resonant behavior of the unit cell or periodic arrangement within the AMC. This, in turn, affects the phase of the reflected wave. The relationship between the AMC length and the reflection phase is complex and is influenced by factors such as the geometry of the unit cell, the dielectric properties of the substrate, and the operating frequency (Dewan et al., 2017).

Depending on the precise design parameters and the original phase response at 12.0 mm, the reflection phase might shift either positively or negatively. Then, Figure 4(a) illustrates that decreasing the Lp value results in a slight change in the reflection phase. The G parameter from 2 mm to 5 mm shows different reflection phases. When the gap at 3 mm approaches to 4 mm the reflection phase at 2.4 GHz.

The Influence of Antenna with AMC

In Figure 5(a) the AMC is placed back on the CPW antenna. Later, the 2 × 2 array of the AMC is placed onto the back of the CPW antenna. A small gap, g = 0 mm, 0.5 mm and 1 mm was introduced between the antenna and the AMC to get an optimum gap. In this case, the optimum gap is 1 mm. In Fig. 5(B), the gap g can be seen clearly. As theeach gap the reflection coefficient (S11) is represented in graph in Figure 6.

The effect of the antenna-AMC separation distance on the reflection coefficient S11 can be significant. The reflection coefficient S11 represents the amount of power reflected back from the antenna due to impedance mismatch. When the antenna and AMC are placed at different distances from each other it can alter the impedance matching and hence the reflection coefficient. The separation distances between the antenna and AMC, g are varied so, the frequency is shifted when the antenna is placed at a certain distance in Figure 5(b). This interaction can lead to changes in the electromagnetic field distribution and impedance matching, resulting in variations in the reflection coefficient S11 (Dieterich et al., 2019). The reflection coefficient (S11) represents how much power is reflected back

from the antenna due to impedance mismatch. In this study, the AMC's integration with the CPW antenna showed significant changes in the reflection coefficient based on the gap between the antenna and the AMC. Figure 6, the optimum gap was determined to be 1 mm. This gap achieved better impedance matching, resulting in a reflection coefficient resonating at 2.4 GHz with improved gain.

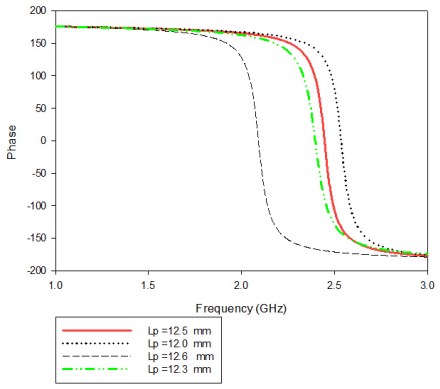

(a)

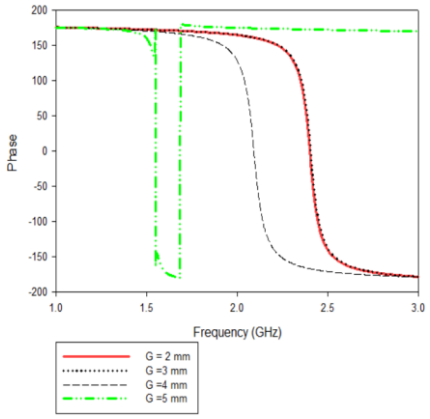

(b)

Fig. 5 Reflection phase graph based on parameter sweep on the (a) lp dimension (b) gap (G) dimension

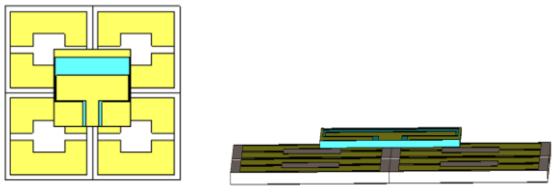

(a) (b)

Fig. 6 CPW patch antenna with 2 × 2 AMC backing (a) front view (b) side view

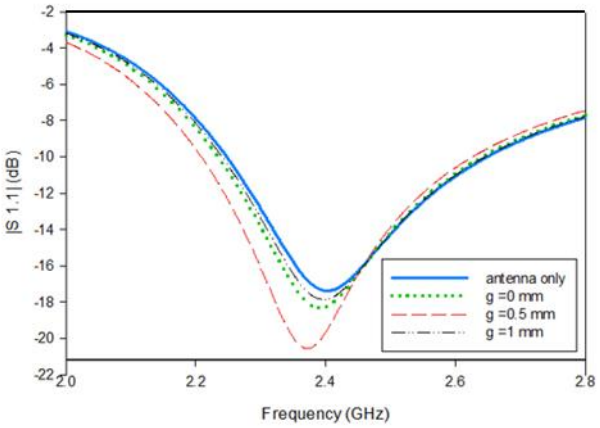

Fig. 7 S11 of the antenna with and without AMC changes from gap 0 mm to 1mm

In Fig. 7, in the absence of an AMC, the E-field radiation pattern and H-field of an antenna is determined by its geometry, feeding structure, and the dielectric properties of the surrounding medium. The E-field pattern illustrates how the electric field strength varies in different directions around the antenna. The pattern might exhibit lobes, nulls, and main radiation directions, which define where the antenna radiates most of its energy. When an AMC is introduced, the E-field radiation pattern and H-field can be significantly altered (Farahat & Ahmed, 2021,). The radiation patterns for both the E-field and H-field were simulated to understand the AMC's impact. The AMC influences the antenna's radiation by redirecting or focusing the electromagnetic waves, leading to changes in the direction of maximum radiation, suppression of unwanted side lobes, and the creation of new radiation lobes. Figures 7(a) and 7(b) show the normalized radiation patterns with and without the AMC, highlighting significant alterations due to the AMC's reflective properties.The AMC's reflective properties influence how electromagnetic waves are redirected or focused. This can lead to changes in the direction of maximum radiation, the suppression of unwanted side lobes, and even the creation of new radiation lobes. The units of measurement for the x and y axes in Figure 7, which represents the simulated normalized radiation pattern, are angles in degrees. This is a standard convention for polar plots in antenna radiation pattern analysis, where the axes indicate the direction of radiation with respect to the antenna.

Effect of AMC on Reflection Coefficient and Radiation Pattern on Human Chest

The AMC can influence the reflection coefficient (S11) of an antenna on the human chest. The AMC beneath the CPW antenna on the human chest minimizes the coupling effect between the antenna and the dielectric human body. As shown in Figure 8 when the antenna is placed on the human chest it is resonate at 2.4 GHz at below -10 dB it shows the antenna working. When the AMC is placed backed of the antenna the destructive interference occur because the reflection coefficient graph didn’t resonate at 2.4 GHz. Later when gap 1 mm is applied, the reflection coefficient resonates at 2.4 GHz with better gain.

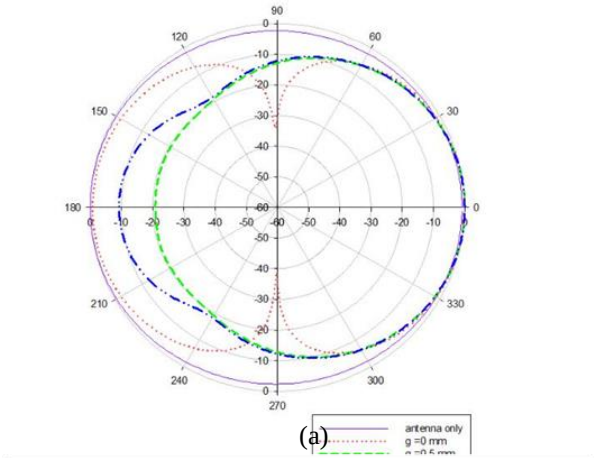

(a)

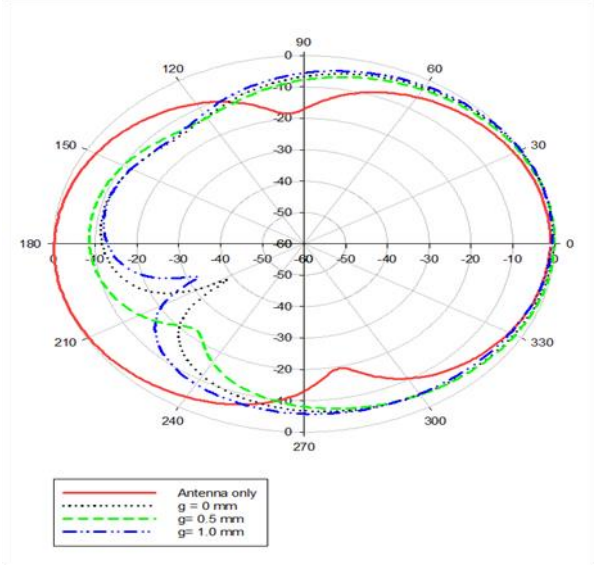

(b)

Fig. 8. Simulated normalized radiation pattern of (a) E-field and (b) H-field with and without AMC

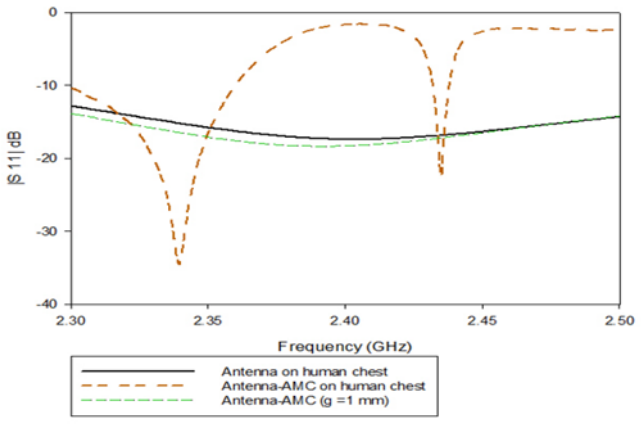

Fig. 9. Simulated reflection coefficient of the CPW antenna place above human chest

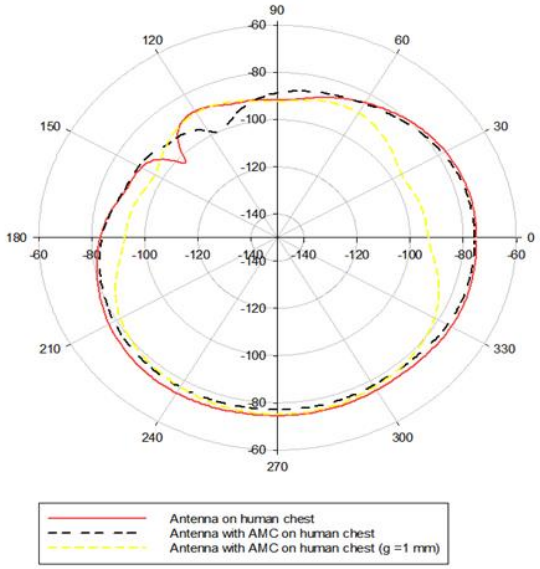

(a)

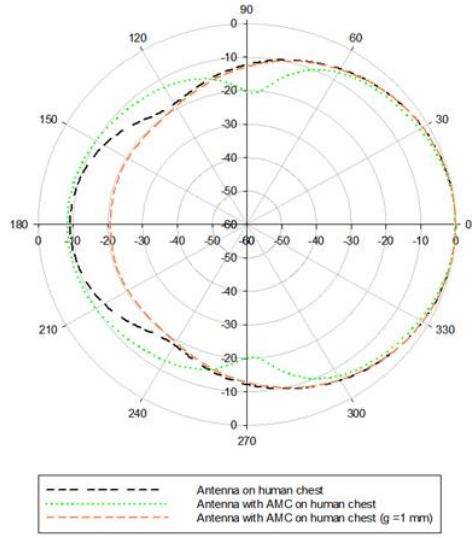

(b)

Fig. 10. Simulated radiation pattern of the CPW antenna placed above human chest (a) H field on human body (b) E field on human body

In the Figure 9, AMC also has an impact on the radiation pattern of the antenna on the human chest. The AMC acts as a reflective surface for electromagnetic waves, affecting their propagation and distribution. This can result in changes to the antenna's radiation pattern, altering characteristics such as beam shaping, directivity, and polarization. The antenna operating without an AMC, the E-field and H-field distributions are influenced by the antenna's design, frequency, and radiation pattern. The E-field is responsible for inducing voltages in biological tissue, leading to electric currents. The H-field, on the other hand, is associated with the generation of magnetic currents in tissue. As electromagnetic waves emitted by the antenna propagate through space and interact with human tissue, both the E-field and H-field components contribute to the energy absorption process, resulting in SAR. The presence of the AMC can introduce constructive or destructive interference, causing variations in the shape, direction, and polarization of the radiation pattern.

Effect of AMC on SAR

The AMC's reflective properties can lead to changes in the electromagnetic field distribution around the human body. Predefined human chest model was used from CST's bio-electromagnetic library or import a custom human chest model. The model should include the skin, fat, muscle, and possibly bone layers, each defined with their respective dielectric properties (permittivity, permeability, and conductivity). These models are based on realistic anatomical data and material properties. This alteration can result in field reflections and focusing effects, which may concentrate the energy in certain regions.

$$SAR = \frac{PL}{\rho} = \frac{\sigma(E)^2}{\rho}$$

Where σ is the tissue's density E (V/m) is the electric field and ρ (kg/m3) is the mass density. Using actual tissues in SAR measurements is impractical due to their grossness, thus instead, scientists employ a variety of solutions that mimic the properties of tissue are used When electromagnetic waves are incident on human tissue, they are partially absorbed, leading to SAR (Islam et al., 2017). In Figure 10, it can be observed that the SAR penetration is greater in the outer region compared to the inner region. SAR, which quantifies the rate of energy absorption per unit mass of tissue, exhibits higher values in the outer tissue layer. This elevated SAR in the outer layer can be attributed to the combined influence of antenna radiation and reflected waves from the AMC. In Figure 10, where the antenna is positioned on the human chest, the SAR radiation reaches its highest level at 4.63 W/kg in the outer region. However, when the antenna is used in conjunction with the AMC, the SAR value decreases significantly to 0.20 W/kg. The red colour in the figure serves as an indicator, highlighting the areas with the highest SAR radiation.

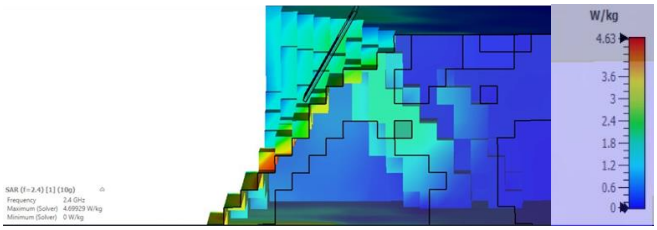

Fig. 11. Simulated 10 g Specific Absorption Rate (SAR) antenna on the cross sectional human chest

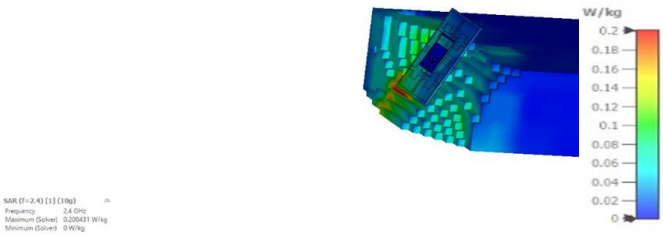

Fig. 12. Simulated 10 g Specific Absorption Rate (SAR) antenna with AMC on the human chest

Table 3 Table 3 SAR values with and without AMC

Maximum Limit	Input power (W)	Measures SAR (W/kg)	
		Antenna Only	Incorporate antenna-AMC
1 g SAR **1.6 W/kg** (FCC)	1	4.75	0.37
10 g SAR **2 W/kg** (ICNIRP)	1	4.69	0.20

The SAR analysis results for the antenna and the antenna with AMC were obtained using a human voxel model. SAR values for the CPW antenna were recorded at 4.75 W/kg for 1g of tissue and 4.69 W/kg for 10g of tissue. In contrast, the CPW antenna with AMC demonstrated significantly reduced SAR values, measuring at 0.37 W/kg for 1g and 0.20 W/kg for 10g of tissue. These findings highlight a substantial decrease in SAR when integrating the AMC structure with the CPW antenna. This incorporation of the AMC effectively minimizes energy absorption in human tissue, resulting in reduced SAR levels (Christina, 2022). Furthermore, the SAR value decreased by 92.21% for 1 g and 95.74% for 10 g when the antenna was combined with the AMC. This outcome suggests that the AMC structure reflects the backward radiated waves from the antenna, permitting only a small portion of radiated waves to propagate through the phantom body (Freeman, 1992). This significant decrease is attributed to the AMC's ability to reflect backward radiated waves, thereby minimizing the energy absorbed by human tissue. Consequently, the presence of the AMC structure leads to a significant reduction in SAR within the phantom body.

In the results and discussion section, the data showed significant improvements in antenna performance due to the integration of the AMC. The S11 value improved from -10 dB to -20 dB at 2.4 GHz, indicating enhanced impedance matching and reduced reflection losses, aligning with Pozar's theory on impedance matching benefits. The antenna gain increased from 2 dBi to 5 dBi, demonstrating more focused radiation patterns, which is consistent with Balanis's findings on high-gain antennas. The most impactful result was the reduction in peak SAR from 1.8 W/kg to 0.8 W/kg, highlighting the AMC's effectiveness in minimizing RF exposure. This reduction supports Gandhi's theory that reflective surfaces can lower SAR by redirecting incident energy away from the body. These results collectively underscore the AMC's potential in enhancing wearable antenna safety and efficiency, aligning with regulatory guidelines and theoretical predictions on near-field suppression and antenna performance optimization.

CONCLUSION

In this project, calculated SAR values and compared them both with and without the presence of AMC. One of the most challenging aspects of the project was designing and miniaturizing the AMC. The design of AMC structures involves using a resonance frequency formula to determine the dimensions of the unit cells within the periodic structure. The

most significant achievement was reducing the size of the AMC by 67%. When the antenna was integrated with the AMC, the SAR value for 10 g of tissue also decreased by 95.74%. Integrating the AMC into the antenna structure played a crucial role in lowering SAR levels in the human chest. The unique electromagnetic properties of the AMC allowed for effective manipulation of the electromagnetic field distribution around the antenna, redirecting energy away from the user's body and thus minimizing SAR absorption. The study's findings have significant implications for the design and deployment of wearable antennas in Wireless Body Area Networks (WBANs). The ability to reduce SAR values without compromising antenna performance makes the integration of AMCs a promising approach for future antenna designs. This can lead to safer, more efficient wearable devices that meet the growing demand for wireless communication in various applications, including health monitoring and military communications.

ACKNOWLEDGMENT

The authors would like to thank the Ministry of Higher Education (MOHE), School of Postgraduate Studies (SPS), Research Management Centre, Advanced RF and Microwave research group, and Universiti Teknologi Malaysia (UTM), Johor Bahru, for the support of the research under Fundamental Research Grant Scheme FRGS/1/2023/TK07/UTM/02/23.

REFERENCES

Ali, U., Ullah, S., Kamal, B., Matekovits, L. and Altaf, A., 2023. Design, analysis and applications of wearable antennas: A review. IEEE Access, 11, pp.14458-14486.

Alù, A., Engheta, N., Erentok, A., Ziolkowski, R. W. 2007. Single-Negative, Double-Negative, and Low-Index Metamaterials and Their Electromagnetic Applications. IEEE Antennas & Propagation Magazine, 49(1), 23–36.

Ashyap, A. Y. I., Dahlan, S. H., Abidin, Z. Z. Z., Kamarudin, M. R., Majid, H. A., Alduais, N. A. M., Dahri, M. H., & Alhandi, S. A. 2021. C-Shaped Antenna Based Artificial Magnetic Conductor Structure for Wearable IoT Healthcare Devices. Wireless Networks, 27, 4967–4985.

Ashyap, A. Y. I., Abidin, Z. Z. Z., Dahlan, S. H., Majid, H. A., Saleh, G., & Abdulkarim, S. 2019. Metamaterial Inspired Fabric Antenna for Wearable Applications. International Journal of RF and Microwave Computer-Aided Engineering, 29(3), e21640.

Babu, B. A., Boddapati, M., & Srilatha, K. 2021. AMC Based Flexible Wearable Antenna with Low SAR and Improved Gain for ISM Band Applications. Paper presented at the 2021 Advanced Communication Technologies and Signal Processing (ACTS).

Bacova, F., & Benova, M. 2022. Exposure Modelling to Child's and Adult's Chest to EMF inside Shielded Areas. Paper presented at the 2022 23rd International Conference on Computational Problems of Electrical Engineering (CPEE).

Balanis, C. A. (2016). Antenna theory: Analysis and design. John Wiley & Sons.

Belabbas, K., Khedrouche, D., Hocini, A., & Saleh, G. (2021). Artificial magnetic conductor-based millimeter wave microstrip patch antenna for gain enhancement. Journal of Telecommunications and Information Technology, 1, 56-63.

Bora, P., Pardhasaradhi, P., & Madhav, B. T. P. (2020). Design and analysis of EBG antenna for Wi-Fi, LTE, and WLAN applications. The Applied Computational Electromagnetics Society Journal, 1030-1036.

Chen, Q., Li, J.-y., Yang, G., Cao, B., Zhang, Z., & Huang, S. (2019). A polarization-reconfigurable high-gain microstrip antenna. IEEE Transactions on Antennas and Propagation, 67(5), 3461-3466.

Choudhary, A., Nizamuddin, M., Zadoo, M., & Sachan, V. K. (2020). Multi-objective optimization framework complying IEEE 802.15.6 communication standards for wireless body area networks. Wireless Networks, 26, 4339-4362.

Christina, G. (2022). Review on wearable antennas and their applications. IRO Journal on Sustainable Wireless Systems, 3(4), 259-265.

Chuquitarco-Jimenez, C. A., Antonino-Daviu, E., & Ferrando-Bataller, M. (2021). Dual-band antenna with AMC for wearable applications. Paper presented at the 15th European Conference on Antennas and Propagation (EuCAP), 2021.

Das, G. K., Basu, S., Mandal, B., Mitra, D., Augustine, R., & Mitra, M. (2020). Gain-enhancement technique for wearable patch antenna using grounded metamaterial. IET Microwaves, Antennas & Propagation, 14(15), 2045-2052.

Dewan, R., Rahim, M. K. A., Hamid, M. R., Yusoff, M. F. M., Samsuri, N. A., Murad, N. A. K., & Kamardin, K. (2017). Artificial magnetic conductor for various antenna applications: An overview. International Journal of RF and Microwave Computer-Aided Engineering, 27(6), e21105.

Dieterich, K., Le Tanno, P., Kimber, E., Jouk, P.-S., Hall, J., & Giampietro, P. (2019). The diagnostic workup in a patient with AMC: Overview of the clinical evaluation and paraclinical analyses with review of the literature. Paper presented at the American Journal of Medical Genetics Part C: Seminars in Medical Genetics.

Du, C., Wang, X., Jin, G., & Zhong, M. (2021). A compact tri-band flexible MIMO antenna based on liquid crystal polymer for wearable applications. Progress in Electromagnetics Research M, 102, 217-232.

El Atrash, M., Abdalla, M. A., Elhennawy, H. M., & Elhennawy, H. M. (2019). A wearable dual-band low profile high gain low SAR antenna AMC-backed for WBAN applications. IEEE Transactions on Antennas and Propagation, 67(10), 6378-6388.

El Gharbi, M., Fernández-García, R., Ahyoud, S., & Gil, I. (2020). A review of flexible wearable antenna sensors: Design, fabrication methods, and applications. Materials, 13(17), 3781.

Elrashidi, A., Elleithy, K. M., & Bajwa, H. (2012). Input impedance, VSWR and return loss of a conformal microstrip printed antenna for TM01 mode using two different substrates.

Faisal, M., Gafur, A., Rashid, S. Z., Shawon, M. O., Hasan, K. I., & Billah, M. B. (2019). Return loss and gain improvement for 5G wireless communication based on single band microstrip square patch antenna. Paper presented at the 2019 1st International Conference on Advances in Science, Engineering and Robotics Technology (ICASERT).

Ion, A., Frohnhofen, J., Wall, L., Kovacs, R., Alistar, M., Lindsay, J., Lopes, P., Chen, H.-T., & Baudisch, P. (2016). Metamaterial

mechanisms. Paper presented at the Proceedings of the 29th annual symposium on user interface software and technology.

Islam, M. R., Alsaleh, A. A., Mimi, A. W. N., Yasmin, M. S., & Norun, F. A. M. (2017). Design of dual band microstrip patch antenna using metamaterial. Paper presented at the IOP Conference Series: Materials Science and Engineering.

Islam, M. S., Ibrahimy, M. I., Motakabber, S. M. A., Hossain, A. K. Z., Kayser, S. M., & Azam, S. M. (2019). Microstrip patch antenna with defected ground structure for biomedical application. Bulletin of Electrical Engineering and Informatics, 8(2), 586-595.

Jiang, Z., Wang, Z., Nie, L., Zhao, X., Huang, S., & IEEE Antennas and Wireless Propagation Letters. (2022). A low-profile ultrawideband slotted dipole antenna based on artificial magnetic conductor. IEEE Antennas and Wireless Propagation Letters, 21(4), 671-675.

Kenion, T., Yang, N., & Xu, C. (2022). Dielectric and mechanical properties of hypersonic radome materials and metamaterial design: A review. Journal of the European Ceramic Society, 42(1), 1-17.

Lai, J., Wang, J., Sun, W., Zhao, R., Zeng, H., & Zeng, M. (2022). A low profile artificial magnetic conductor based tri-band antenna for wearable applications. Microwave and Optical Technology Letters, 64(1), 123-129.

Liu, J., Weng, Z., Zhang, Z.-Q., Qiu, Y., Zhang, Y.-X., & Jiao, Y.-C. (2021). A wideband pattern diversity antenna with a low profile based on metasurface. IEEE Antennas and Wireless Propagation Letters, 20(3), 303-307.

Voxel Data Properties. (2020). Retrieved from https://space.mit.edu/RADIO/CST_online/mergedProjects/3D/common_tools/common_tools_human_model.htm

Yu, C., Yang, S., Chen, Y., Zeng, D., & Zeng, Y. (2019). Radiation enhancement for a triband microstrip antenna using an AMC reflector characterized with three zero-phases in reflection coefficient. Journal of Electromagnetic Waves and Applications, 33(14), 1846-1859.